CONF-790646--4

INTERNATIONAL COLLOQUIUM ON IRRADIATION TESTS

FOR REACTOR SAFETY PROGRAMMES

MASTER

JUNE 25-28, 1979

PETTEN, THE NETHERLANDS

THE LINEAR VARIABLE DIFFERENTIAL TRANSFORMER AND ITS USES FOR IN-CORE FUEL ROD BEHAVIOR MEASUREMENTS

J. R. Wolf

Idaho National Engineering Laboratory
EG&G Idaho, Inc.
P.O. Box 1625
Idaho Falls, Idaho 83401
United States of America

THE LINEAR VARIABLE DIFFERENTIAL TRANSFORMER AND ITS USES FOR IN-CORE FUEL ROD BEHAVIOR MEASUREMENTS

J. R. Wolf

Idaho National Engineering Laboratory
EG&G Idaho, Inc.
P.O. Box 1625
Idaho Falls, Idaho 83401
United States of America

ABSTRACT

The linear variable differential transformer (LVDT) is an electromechanical transducer which produces an ac voltage proportional to the displacement of a movable ferromagnetic core. When the core is connected to the cladding of a nuclear fuel rod, it is capable of producing extremely accurate measurements of fuel rod elongation caused by thermal expansion.

The LVDT is used in the Thermal Fuels Behavior Program at the U.S. Idaho National Engineering Laboratory (INEL) for measurements of nuclear fuel rod elongation and as an indication of critical heat flux and the occurrence of departure from nucleate boiling. These types of measurements provide important information about the behavior of nuclear fuel rods under normal and abnormal operating conditions.

The objective of this paper is to provide a complete account of recent advances made in LVDT design and experimental data from in-core nuclear reactor tests which use the LVDT.

NOMENCLATURE

b	length of primary coil
m	length of each secondary coil
r_i	inside coil diameter
r_o	outside coil diameter

d	spacing between coils
L_a	length of core
H	magnetic field strength
B_{L1}, B_{L2}	magnetic leakage flux densities for Paths I and II
B_{LP}	magnetic leakage flux densitites through primary coil
L1, L2	length of magnetic Paths I and II
LP	length of magnetic path in primary coil
n_p	number of primary turns
n_s	number of secondary turns
Ip	primary current (rms)
f	excitation frequency
e_1, e_2	induced voltages in secondary coil one and two
X_1, X_2	core penetration distance
e	differential voltage of secondary coils
X	core displacement
K_1	sensitivity
K_2	nonlinearity factor
ε	nonlinearity term
X_o	distance
y	integration variable
μo	magnetic permeability
Φ	total magnetic flux

INTRODUCTION

The LVDT consists of a movable ferromagnetic core and three coils; a primary and two equally spaced, identical secondaries. When the primary coil is excited by an alternating current, the changing magnetic field caused by this current induces a voltage in each of the secondaries. The motion of the movable ferromagnetic coil, which is connected to the object whose displacement is to be measured, varies the mutual inductance between the primary and secondary coils. The increased or decreased coupling has the effect of changing the induced voltage in the secondary coils and, as a result, the output of the transducer.

In normal operation, the secondaries are connected in series opposition; therefore, the net transducer output is the difference between the individual secondary voltages. When the core is centered between the secondary coils, the magnetic coupling between the coils is equal and the differential output is zero. This position is referred to as the null position. As the core moves from the null position toward one coil, the induced voltage is increased in that coil while the coil which the core is moving away from undergoes a reduction in induced voltage. This effect produces a differential voltage output which is a linear function of transformer core displacement.

The objective of the Thermal Fuels Behavior Program (TFBP) is to determine the performance levels of nuclear fuel rods under a variety of normal and abnormal operating conditions. These data are important to the United States Nuclear Regulatory Commission's Reactor Safety Program.

During nuclear reactor operation, the core of the LVDT is connected to the bottom of the fuel rod cladding. As the temperature of the fuel rod increases, thermal expansion causes the fuel rod to elongate and the LVDT core to be displaced. The transducer output is then a linear function of the cladding elongation. Departure from nucleate boiling (DNB) occurs when there is a mismatch between core power and coolant. The excess core power causes the fuel rod temperature to increase until a critical heat flux is reached. Under these conditions, the rod passes from a state of nucleate boiling into film boiling. This departure from nucleate boiling is detected by the LVDT as a sudden increase in fuel rod cladding elongation. This is the result of a thermal expansion of the cladding due to a rapid temperature increase caused by the film boiling conditions.

This paper concentrates on both the theoretical and experimental aspects of the LVDT. An analytical model is developed which gives a closed-form expression for the differential voltage output of the LVDT. The materials used in the construction of the device are also discussed. Since the LVDT is essentially an impedance device, its output is strongly sensitive to temperature. Signal conditioning, which eliminates this temperature sensitivity, is described.

Finally, experimental in-core data from the TFBP are presented which show that the LVDT is capable of providing accurate fuel rod elongation measurements as well as indicating the onset of DNB.

THEORY OF OPERATION

The analytical expression for the differential voltage output can be obtained by modeling the LVDT as shown in Figure 1, where the primary coil is of length b and the two identical secondaries are each of length m. The coils have an inside diameter of r_i and an outside diameter of r_o. Spacing between the coils is d and the length of the core is L_a. The thickness of the coil form is neglected in this analysis. The nomenclature used is presented at the beginning of the paper.

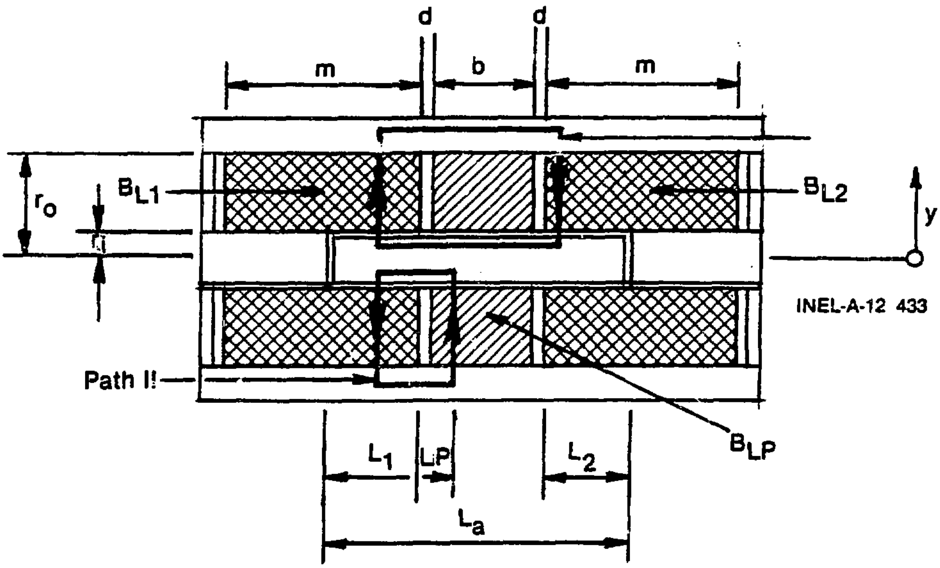

Fig. 1 Linear variable differential transformer model.

The integral form of Ampere's Law[1] can be used to obtain an expression for the magnetomotive force and leakage flux for Paths I and II of Figure 1[2].

For Path I:

$$H \cdot dL = \mu o\ n_p\ Ip = \int_{ri}^{ro} (B_{L1} - B_{L2}) \frac{r_i}{y}\, dy \qquad (1)$$

or

$$B_{L1} - B_{L2} = \frac{4\pi\, n_p\, Ip}{10^7\, r_i \ln(r_o/r_i)} \tag{2}$$

and for Path II:

$$B_{LP} - B_{L1} = \frac{4\pi\, LP\, n_p\, Ip}{10^7\, r_i b \ln(r_o/r_i)}\ . \tag{3}$$

If H and the path element dL are perpendicular, then

$$H \cdot dL = 0.$$

In general

$$L1\, B_{L1} + \int_0^L B_{LP}\, dLP + L2\, B_{L2} = 0 \tag{4}$$

or

$$B_{L1} = -B_{L2}\left[\frac{2L2+b}{2L1+b}\right]. \tag{5}$$

Through substitution from Equation (2), the leakage flux densities for Paths I and II become

$$B_{L1} = \frac{2L2+b}{L_a}\left[\frac{2\pi\, n_p\, Ip}{10^7 r_i \ln(r_o/r_i)}\right] \tag{6}$$

$$B_{L2} = \frac{-2L1+b}{L_a}\left[\frac{2\pi\, n_p\, Ip}{10^7 r_i \ln(r_o/r_i)}\right]. \tag{7}$$

The induced voltage for each coil can now be calculated using Equations (6) and (7), where Φ is the flux linking an elemental coil of width dX_1 and distance X^1 from the primary. If the core penetrates a distance X_1 and the number of turns on the secondary coil is n_s, then the total number of turns in the elemental coil is $\frac{n_s\, dX^1}{m}$ [3].

The flux linking the primary and secondary coil is $\Phi_X = 2\pi r_1 X^1$. The total flux turns can be found by integrating each elemental coil over the distance the core penetrates into the secondary coil. The total flux turns which are linked together in the secondary coil become

$$\int_0^{X^1} \frac{\Phi X^1 n_s}{m} dX^1 = \frac{2\pi r_i B_{L1} n_s}{m} \int X^1 dX^1 \tag{8}$$

$$= \pi r_i B_{L1} n_s X_1^2 .$$

Through application of Faraday's Law[4], the induced voltage in each secondary becomes

$$e_1, e_2 = -n_p \frac{d\Phi}{dt} .$$

With a sinusoidal excitation current Ip (rms) and of frequency f in the primary, the rms voltage e_1 induced in secondary Coil 1 is

$$e_1 = \frac{4\pi^3}{10^9} \left[\frac{fIp\ n_p\ n_s\ (2L2 + b)}{\ln\left(\frac{r_o}{r_i}\right) mL_a} \right] X_1^2 \tag{9}$$

and for Coil 2

$$e_2 = \frac{4\pi^3}{10^9} \left[\frac{fIp\ n_p\ n_s\ (2L1 + b)}{\ln\left(\frac{r_o}{r_i}\right) mL_a} \right] X_2^2 . \tag{10}$$

The differential voltage $e = e_1 - e_2$ can be written as

$$e = K_1 X (1 - K_2 X^2) \tag{11}$$

where

$X = (X_1 - X_2)/2$ in the core displacement, K_1 is the sensitivity e/X, and $X_o = (X_1 + X_2)/2$.

The quantity K_1 is given by

$$K_1 = \frac{16\pi^3\ fIp\ n_p\ n_s\ (b + 2d + X_o)\ X_o}{10^9 \ln\left(\frac{r_o}{r_i}\right) m\ L_a} \tag{12}$$

and

$$K_2 = \frac{1}{(b + 2d + X_o)\ X_o} .$$

The quantity K_2 is the nonlinearity factor in Equation (11). If $K_2 = 0$, then the induced secondary voltage is a linear function of the core displacement X. A nonlinear term ε can also be defined as

$$\varepsilon = K_2 X^2. \tag{13}$$

For any given accuracy and maximum displacement, the overall length of the LVDT can be shown to be a minimum for $X_0 = b$ [5]. If the assumption is made that the core does not emerge from the secondary coils and that the quantity 2d is small compared with b, Equations (11) and (13) can be combined to produce an analytical form for the LVDT differential voltage output

$$e = \frac{16\pi^3 \, fIp \, n_p \, n_s \, 2b}{10^9 \, \ln\left(\frac{r_o}{r_i}\right) 3m} \left(\frac{1-X^2}{2b^2}\right). \tag{14}$$

Equation (14) can be used as a basis for a parametric study to determine LVDT sensitivity to various design parameters, or as a means of assessing actual performance of the device. This equation was used extensively in a parametric study for the design of a temperature compensating signal conditioner.

DESIGN AND OPERATING CHARACTERISTICS

The LVDT is used to provide in-core measurements of fuel rod cladding elongation and detection of DNB for the TFBP. It must be able to withstand the nuclear core and coolant conditions for several hundred hours. Typical in-core conditions in the Power Burst Facility (PBF) reactor where these tests are conducted are 15.5 MPa, 602 K, and 10^{19} nvt.

These conditions put several limitations and restrictions on the type of materials used in the design. Water at pressurized water reactor (PWR) temperatures and pressures is an extremely corrosive medium. Few materials have the necessary corrosion resistance and strength at these elevated temperatures and pressures. In addition, the high in-core radiation environment excludes many materials with high neutron cross sections because of activation problems. The ferromagnetic core must be made of a material which will not only withstand the core environment, but will also have a magnetic curie temperature which is high enough to allow retention of magnetic properties.

Figure 2 shows a typical LVDT as used in the PBF. Table I is a summary of the materials used in the construction of the transducer components. The materials which are currently used in the LVDT have performed satisfactorily during the entire Thermal Fuels Behavior Program.

The LVDT, in its present configuration, has a linear design range of ±0.012 m, or 0.0254-m total displacement travel. The linearity of the device is 0.02%, where the linearity is defined as[6]:

$$\text{Linearity} = \frac{\text{maximum deviation from a least-squares fit straight line}}{\text{full range output}} .$$

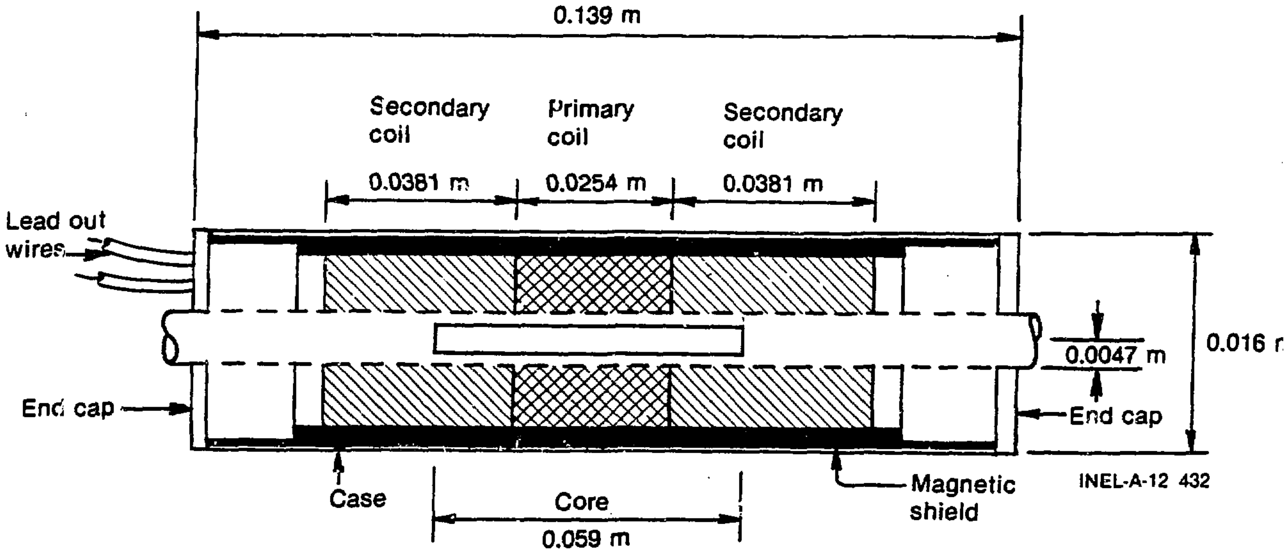

Fig. 2 LVDT used in the Power Burst Facility reactor.

Response time for a 10 to 90% rise time is 0.003 seconds. Under normal operating conditions, the LVDT is presently excited by a commercial carrier amplifier at 3000 Hz with 3.0 volts rms.

TABLE I

LVDT CONSTRUCTION MATERIALS

Component	Material
Core	17-4PH stainless steel
Case	304 stainless steel
Coil form	304 stainless steel
End caps	304 stainless steel
Magnetic shield	Silicon steel-Ams 7714M36
Coil wire	Secon Alloy 406 with Type E high temperature insulation
Primary and secondary leadwire	Stainless steel sheath, nickel-clad copper
Cements	Yellow cerro ceramic cement

Table II summarizes the design and performance specifications of the LVDT used in the PBF.

For the LVDT to operate in a nuclear environment, its design must be immune to radiation effects. Measurements using the LVDT have been made for a large number of tests with constant radiation levels. During these tests, no evidence has been seen that the performance was degraded by radiation effects.

TABLE II

DESIGN AND PERFORMANCE SPECIFICATIONS

Design Specifications	
Primary coil length	0.0254 m
Secondary coil length	0.0381 m
Core length	0.0381 m
Number of primary coil turns	615 to 655
Number of secondary coil turns	615 to 655
Case length	0.139 m
Case diameter	0.016 m
Performance Specifications	
Linear range	± 0.0127
Linearity	0.02%
Sensitivity	12.99 V/m
Accuracy	0.0001 m
Response time	0.003 s
Excitation frequency	3000 Hz
Excitation voltage	3 volts rms
Normal operating temperature	602 K
Maximum operating temperature	741 K
Normal operating pressure	15.5 MPa

TEMPERATURE SENSITIVITY AND SIGNAL CONDITIONING

Proper conditioning of the LVDT differential output signal is essential. The LVDT is basically an impedance device and, without special temperature compensating electronics, exhibits a large temperature sensitivity which causes large uncertainties to be added to the measurement.

When the operating temperature of the LVDT is increased, a family of displacement versus output curves is generated. For a full-scale displacement as shown in Figure 3, an 18.3% displacement error occurs for the same voltage output over the temperature range of 280 to 602 K, using the commercial carrier amplifier for signal conditioning.

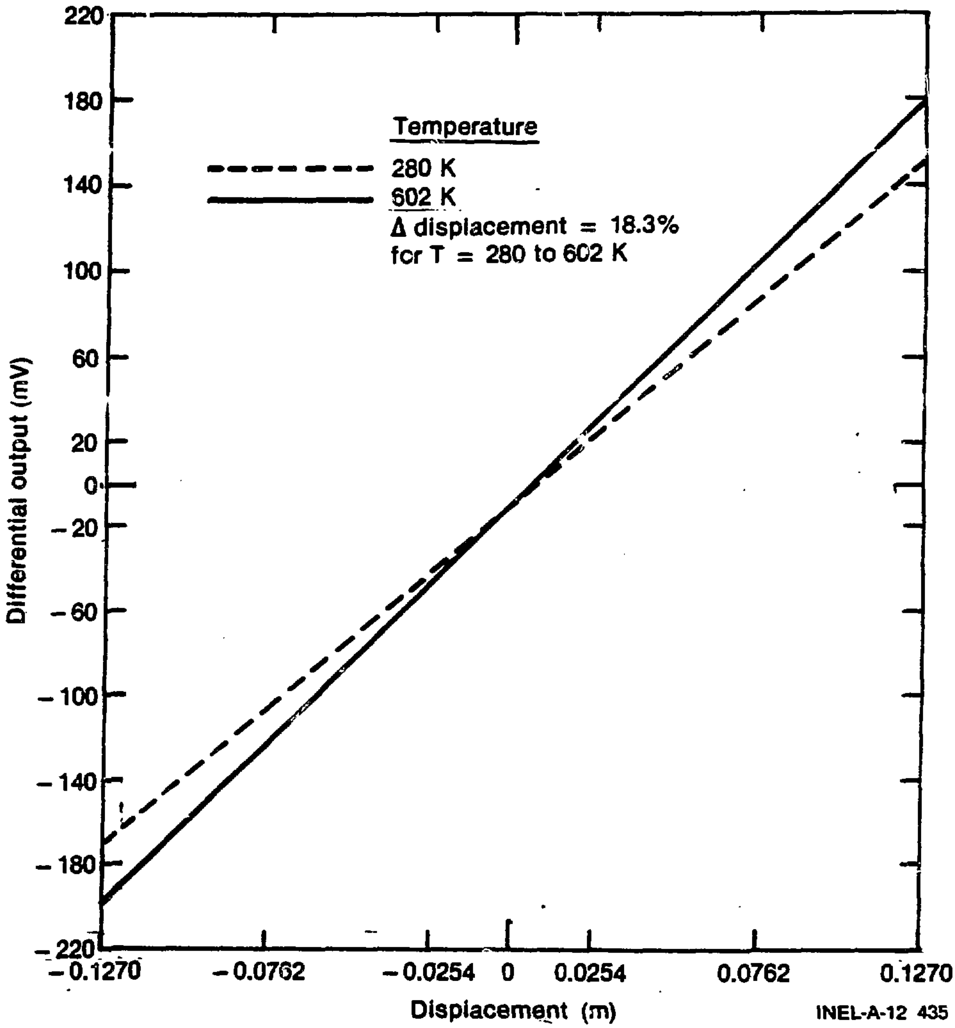

Fig. 3 Temperature sensitivity of the LVDT for temperatures of 280 and 602 K.

Several reasons exist for this effect. First, the magnetic permeability of the core changes as a function of temperature. As the permeability changes, so does the mutual inductance between the primary and secondaries. This change in mutual inductance in turn changes the induced voltage in the secondaries, which produces a different voltage output for the same core displacement. The primary coil resistance is also a function of temperature. As the resistance changes due to temperature, the constant voltage oscillator produces less current with which to excite the primary coil. This lower current produces a smaller coupling magnetic field and less output from the device. Almost all commercial LVDT signal conditioners are constant voltage designs and provide no temperature compensation.

In addition to the lack of temperature compensation, commercial signal conditioners operate on a phase sensitive detection principle. During the LVDT calibration process, the core is set at its maximum displacement and the phase of the output signal is adjusted to produce a maximum signal.

The voltage-displacement calibration is only valid for a given phase setting. Any other setting produces an incorrect reading. Therefore, if an LVDT calibration curve is to produce accurate results, the LVDT must be used with the exact signal conditioner with which it was calibrated.

If, during actual reactor use, a signal conditioner should fail, the LVDT core cannot be brought back to a known position to properly adjust the phase on another signal to match the original calibration data. Also, in TFBP usage, the LVDT is extremely radioactive after a test, which makes posttest calibration with the replacement conditioner impossible. As a result of signal conditioner failure, all information from the LVDT is lost for the remainder of the test.

Over the past few years, several methods have been proposed to eliminate the phase sensitive detection and temperature sensitivity problems associated with all LVDTs.

In 1972, K. Ara of the Japanese Atomic Energy Research Institute proposed a method to modify the type of signal conditioning commonly used with LVDTs[7]. Ara's hypothesis was that temperature compensation could be achieved by holding the sum of the secondary coil voltages constant. Then, for any displacement

$$\frac{e_1 - e_2}{e_1 + e_2} = \text{constant}$$

where $e_1 - e_2$ is the differential secondary voltage which is proportional to the core displacement. This approach also has the advantage of not being phase sensitive. Only the amplitude of the signal need be measured.

In order to achieve this type of temperature compensation, a prototype LVDT signal conditioner has been developed at the INEL using this principle. Figure 4 illustrates a block diagram for the LVDT signal conditioning system.

A brief description of the block diagram is as follows. The 1.5-kHz sinewave LVDT output voltages e_1 and e_2 are input to a differential amplifier and summing amplifier. The signal from the differential amplifier is conditioned to provide the dc output voltage. The signal from the summing amplifier is feedback for the regulator that maintains the sum voltage constant.

The differential voltage travels first into a gain amplifier and from there to a peak sampler. The peak sampler samples and holds the positive peaks of the sine wave. The output of the sample hold circuit goes to a deadband clamp, the function of which is to clamp the signal to ground when the differential signal voltage is too small to sample peaks. Outside the deadband, this circuit provides a convenient place to introduce offset. The output of the peak sampler and the deadband clamp is a dc voltage that is always positive. The inverting-noninverting amplifier provides an inversion when the core is displaced at one end of the LVDT and leaves the output noninverted when the core is at the other end of

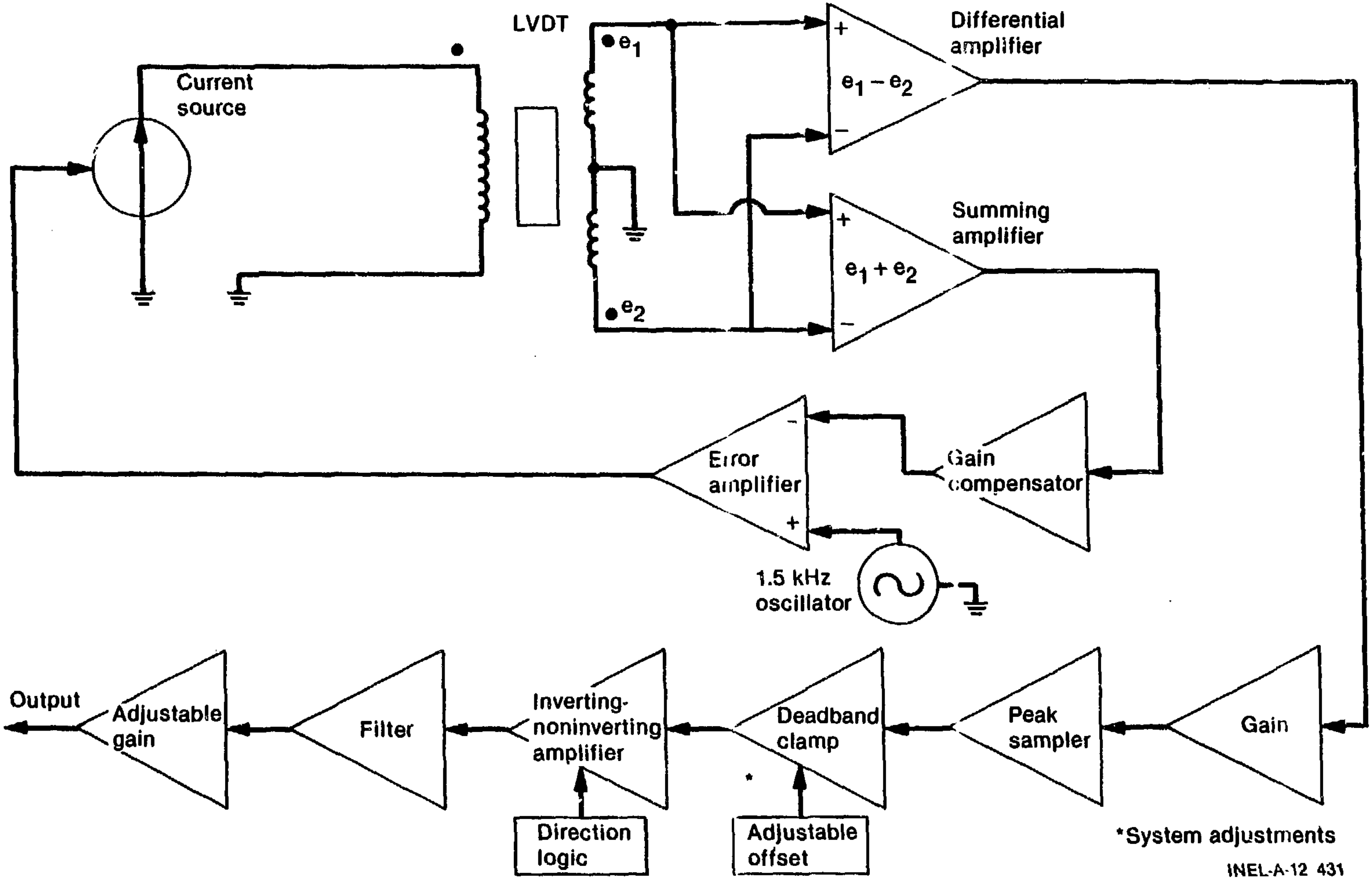

Fig. 4 LVDT temperature compensating electronics block diagram.

the LVDT. The direction of the displacement logic provides the proper signal to the inverting-noninverting amplifier. The signal then passes to a two-pole, low pass filter, with a break frequency of about 8 kHz, where switching noise is filtered out. The signal then travels to an adjustable gain amplifier where the full-scale range can be set. The output of the adjustable gain amplifier is a dc output voltage proportional to displacement.

The sum voltage passes from the sum amplifier to a gain and compensation amplifier and then to a differential error amplifier where the feedback is subtracted from a reference 1.5-kHz sinewave and the resulting error signal is sent to the current driver. The current driver modulates its output proportional to the error signal fed into it. The overall effect is that the control loop tries to hold the sum voltage constant, relative to the reference sinewave.

Laboratory tests have been conducted which show that this type of temperature compensation is capable of removing LVDT temperature sensitivity. An LVDT was connected to a prototype compensating signal conditioner and placed in an oven. Tests were conducted at temperatures of 280 and 602 K. The data from these tests are shown in Figure 5. The temperature sensitivity of the LVDT has been reduced from 18.3 to 3.1% for a full-scale displacement. Depending on actual test requirements, a 3% of full-scale temperature sensitivity may be acceptable. If so, then the LVDT calibration which requires data taken at a number of temperatures could be simplified.

BURST RADIATION EFFECTS

The LVDT has been used in a large number of in-core tests and there has been no evidence of a degradation of performance due to radiation effects caused by normal operation. Until recently, these were the only type of radiation conditions under which the LVDT was required to operate.

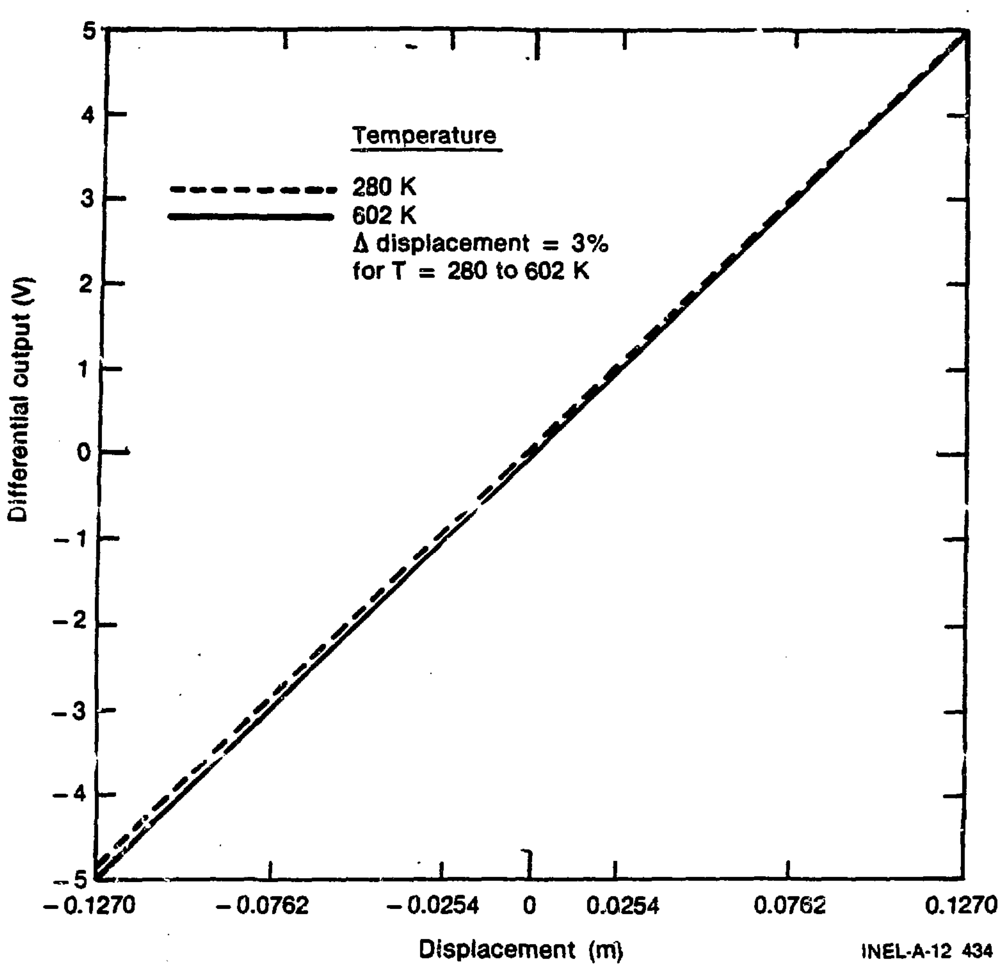

Fig. 5 Temperature sensitivity of the LVDT using compensating signal conditioning.

The Reactivity Initiated Accident Test Series conducted by the TFBP requires that the LVDT be capable of operating under not only steady state radiation conditions, but also under high intensity burst radiation.

The objectives of the RIA Test Series are to determine fuel failure thresholds, modes, and consequences as functions of energy depositions, irradiation history, and fuel rod design. For the RIA Test Series, the pressure, temperature, and flow rate of the coolant are typical of the hot startup conditions in commercial boiling water reactors (BWRs). These conditions were selected to simulate the coolant conditions of the most severe RIA postulated, the BWR control rod drop accident during hot startup conditions[8].

One of the major objectives of the RIA Scoping Tests (RIA-ST) was to determine whether the standard PBF fuel rod instrumentation was sensitive to burst radiation. After the normal power calibration and fuel rod conditioning were completed, a series of burst tests was performed.

To initiate the power burst, all four transient rods were ejected at a velocity of about 9.5 m/s. The burst was largely self-terminating because the PBF driver core and fuel were designed with a Doppler reactivity feedback capable of terminating the burst without primary dependence on mechanical systems. All eight control rods were completely inserted into the driver core to provide mechanical shutdown of the reactor 0.09 second after a 16 500-MW power burst.

To determine short burst radiation effects on the design and performance of the LVDT, a unit was mounted in the reactor test assembly. The core was welded in place at a displacement of 0.0625 m. With the core immobile, radiation effects could be distinguished from those caused by thermal expansion.

As can be seen from Figure 6, no change in output occurred due to the intense radiation from this type of power burst[8]. This test proved that the LVDT, which was previously known to be insensitive to steady state radiation, is also insensitive to short bursts at extremely intense radiation levels.

EXPERIMENTAL IN-CORE FUEL ROD CLADDING ELONGATION MEASUREMENTS

The LVDT is a standard instrument used in all TFBP tests. Data are presented from a recent power-cooling-mismatch test (Test PCM-2) in which the LVDT was used for fuel rod elongation measurements and the detection of DNB. This test, like all tests in the Thermal Fuels Behavior Program, was conducted in the Power Burst Facility.

The PBF reactor is contained in an open tank reactor vessel and consists of a driver core and a flux trap. A pressurized water coolant flow loop provides a wide range of coolant conditions in the flux trap test space.

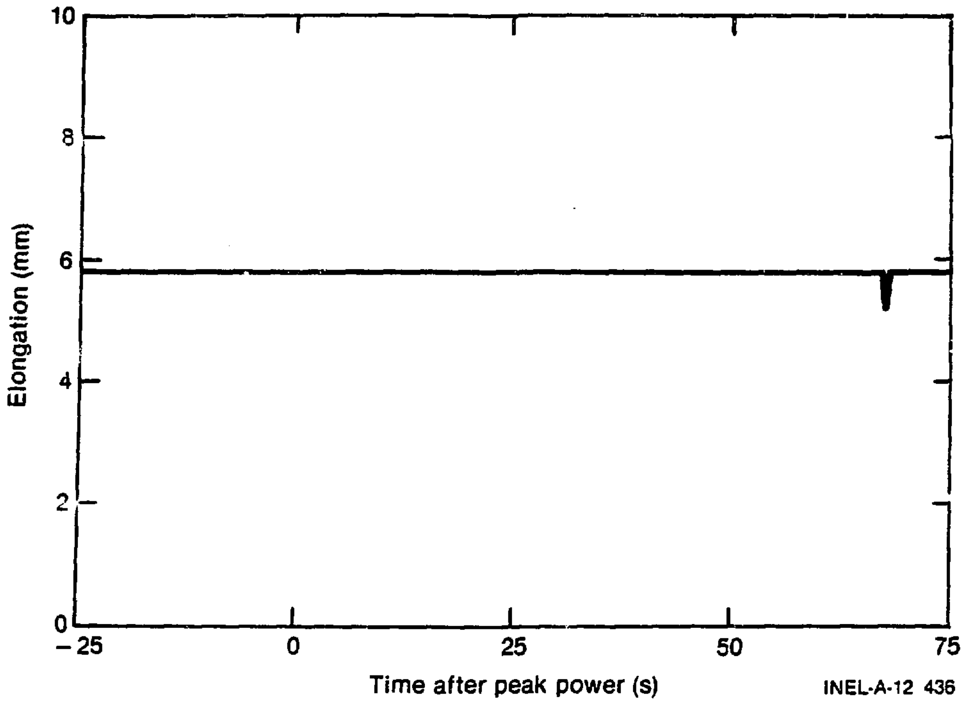

Fig. 6 Radiation sensitivity of the LVDT for RIA Scoping Test.

The PBF core is a right-circular annulus, 1.3 m in diameter and 0.91 m in length, enclosing a centrally located vertical flux trap, 0.21 m in diameter. This core has been designed for steady state and power burst operation. The core contains eight control rods for reactivity control during steady state operation. During power burst operation, the control rods and four additional transient rods dynamically control reactivity. Each of the control and transient rods consists of a stainless steel canister which contains a cylindrical annulus of boron carbide and is operated in an air-filled shroud.

The center of the PBF core is the flux trap region used for experiments. An in-pile tube (IPT) fits in this vertical test space and contains the test train assembly. The IPT is a thick-walled, Inconel 718, high strength pressure tube designed to contain the steady state operating pressure and any pressure surges from test fuel rod failures. It is also designed to safely contain test failures such as cladding failure, gross fuel melting, fuel-coolant interactions, fuel failure propagation, fission product release, and metal-water reactions, and thereby prevent any damage to the driver core.

A flow tube is positioned inside the IPT to direct the coolant flow. Coolant flow enters the top of the IPT above the reactor core and flows down the annulus between the IPT wall and the flow tube. The flow reverses at the bottom, passes up through the test train, and exits above the reactor core at the IPT outlet. The flow tube consists of an upper stainless steel section, a center zircaloy-2 section for neutron economy in the test fuel, and a lower catch basket section for a heat sink and collection of fuel fragments.

In normal operation, the LVDT is positioned at the bottom of the test assembly. Extension rods are used to provide contact from the LVDT core to the bottom of the fuel rod cladding.

During Test PCM-2, four individual rods were tested simultaneously in the PBF in-pile tube. The purpose of this test was to investigate post-DNB behavior of zircaloy clad PWR fuel rods. Departure from nucleate boiling was achieved by decreasing the coolant flow while maintaining constant rod power.

A reactor power calibration was performed at the beginning of the test. This calibration provides a known operating condition in which the level of instrument performance can be determined. Figure 7 shows fuel rod elongation versus peak power for the steady state portion of the power calibration sequence. After the steady state power calibrations were completed, eight separate flow reductions to produce DNB were performed.

Figure 8 shows data taken for Rod UTA-0008 during the eighth DNB cycle[9]. Both the cladding elongation and cladding surface temperature are shown for a position 0.635 m from the bottom of the rod. A definite slope change is shown at 28 380 seconds in Figure 8. At this time the fuel rod experienced a critical heat flux and passed from a nucleate

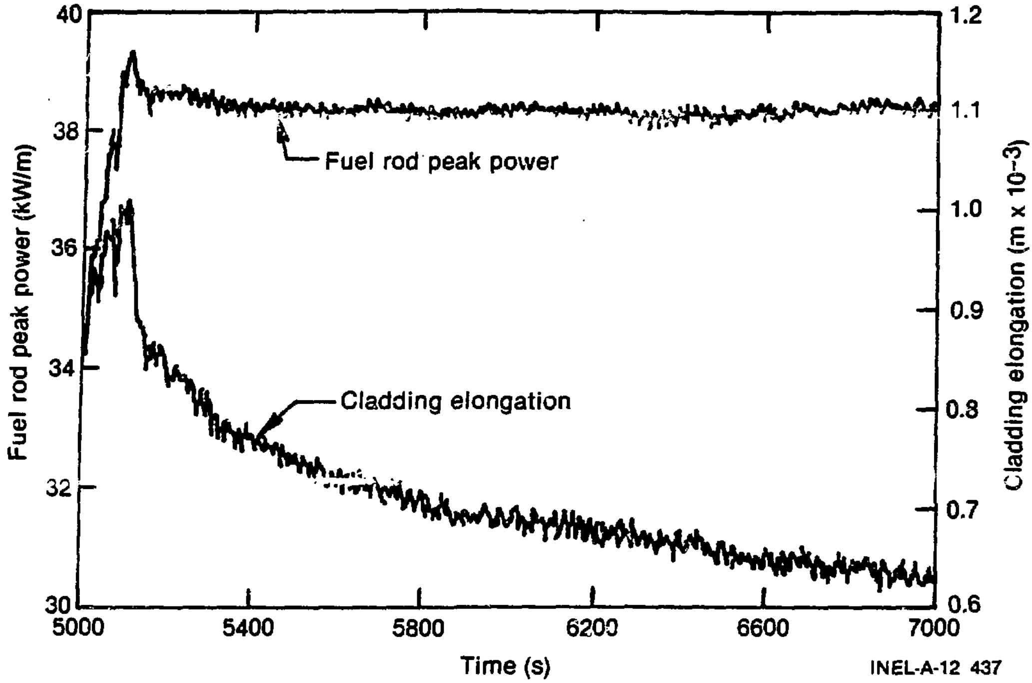

Fig. 7 Fuel rod peak power and cladding elongation as functions of time for Rod A-0014 during steady state operation in power calibration phase of Test PCM-2.

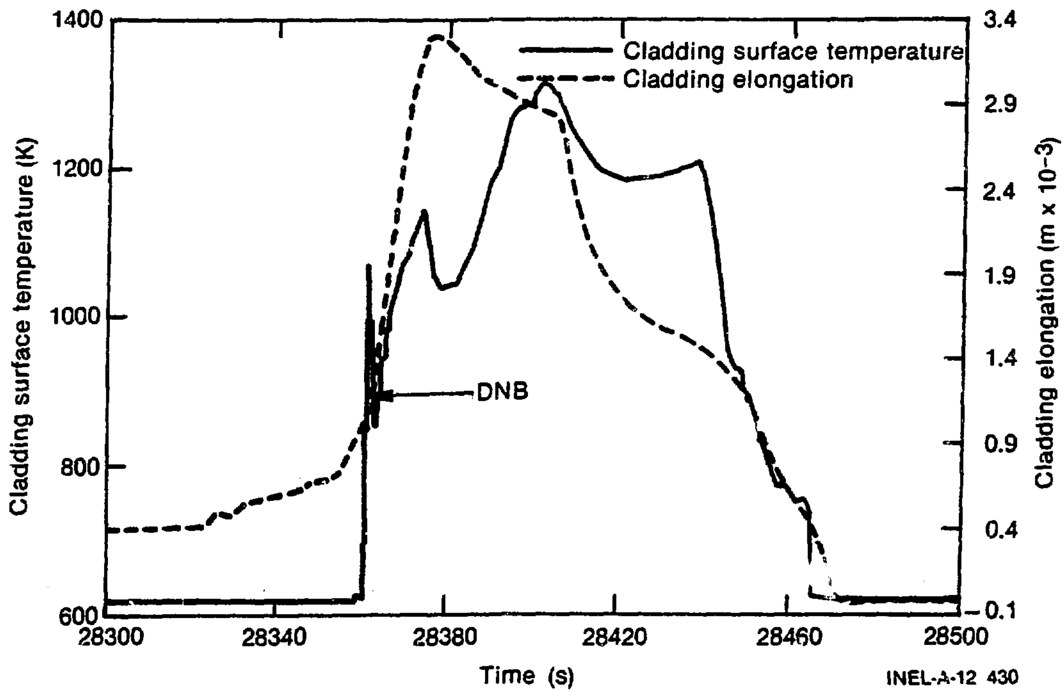

Fig. 8 Cladding surface temperature and cladding elongation as functions of time for Rod UTA-0008 during the final DNB cycle of Test PCM-2.

boiling condition to a condition of film boiling. Also at this time, the fuel rod temperature increased dramatically and a rapid thermal expansion of the cladding resulted. The LVDT measurement showed a maximum cladding elongation of 0.0029 m and a 145-second DNB duration. At this time during the test, the coolant flow was increased and a nucleate boiling condition was again established. Under these flow conditions, the rod rapidly cooled and steady state operation was again achieved as the fuel rod cooled to its steady state operating temperature and the cladding returned to its free thermal expansion value of 0.0008 m. After all fuel rods had returned to normal conditions, the test was terminated.

As can be determined from the data presented in Figure 8, the LVDT is capable of making accurate fuel rod cladding elongation measurements and can also act as an indicator of when a DNB condition exists.

CONCLUSION

The LVDT has been shown to be a reliable and consistent instrument for in-core fuel rod measurements. It remains operational in a PWR environment for extended periods of time.

The self-compensating signal conditioning developed for the LVDT has eliminated the temperature sensitivity problem which usually affects these devices.

The accuracy and response of the LVDT make it an ideal instrument for measuring fuel rod cladding elongation and DNB occurrence. The LVDT is also one of the few instruments which is unaffected by both steady state and intense, short burst radiation.

REFERENCES

1. S. S. Atwood, Electric and Magnetic Fields, New York: John Wiley and Sons, 1949.

2. H. K. Neubert, Instrument Transducers, Oxford, England: Clarendon Press, 1963.

3. D. Halliday and R. Resnick, Physics, New York: John Wiley and Sons, 1966.

4. W. Scott, The Physics of Electricity and Magnetism, New York: John Wiley and Sons, 1966.

5. P. D. Atkinson and R. W. Hynes, "Analysis and Design of a Linear Variable Differential Transformer," Elliott Journal (London), 2 (1954) pp 144-151.

6. E. Herceg, Handbook of Measurement and Control, Pennsauken, New Jersey: Schaevitz Engineering Company, 1976.

7. K. Ara, IEE Transactions on Instruments and Measurements, IM-21, 3 (August 1972) pp 249-255.

8. C. Zimmerman and R. McCormick, Experiment Data Report for Test RIA-ST (Reactivity Initiated Accident Test Series), NUREG/CR-0473, TREE-1235 (March 1979).

9. Z. R. Martinson and R. K. McCardell, Power-Cooling-Mismatch Test Series PCM-2 Test Results Report, TREE-NUREG-1038 (February 1978).